Purification and molecular characterization of the NAD$^+$-dependent acetaldehyde/alcohol dehydrogenase from *Entamoeba histolytica*

Iris BRUCHHAUS and Egbert TANNICH*

Bernhard Nocht Institute for Tropical Medicine, Bernhard Nocht Str. 74, 20359 Hamburg, Germany

A bifunctional 95 kDa polypeptide (EhADH2) harbouring acetaldehyde dehydrogenase and alcohol dehydrogenase activities was purified to homogeneity from trophozoite extracts of the protozoan parasite *Entamoeba histolytica*. Kinetic studies revealed that the enzyme utilizes NAD$^+$ rather than NADP$^+$ as cofactor. K_m values for acetyl-CoA, acetaldehyde and ethanol were found to be 0.015, 0.15 and 80 mM respectively in the presence of 0.2 mM NAD$^+$. The primary structure of EhADH2 as deduced from respective amoebic DNA sequences showed striking similarity to the trifunctional AdhE protein of *Escherichia coli* and the bifunctional AAD protein of *Clostridium acetobutylicum*. Alignment with a number of aldehyde dehydrogenases and alcohol dehydrogenases from various species suggested that the two catalytic functions of EhADH2 are located on separate parts of the molecule. By cross-linking experiments and electron-microscopic analysis, native EhADH2 was found to be organized in a homopolymeric fashion consisting of more than 20 associated promoters which form rods about 50–120 nm in length.

INTRODUCTION

The parasitic protozoan *Entamoeba histolytica* is the causative agent of human amoebiasis. It may cause life-threatening diseases such as haemorrhagic colitis or extraintestinal abscesses. It has been estimated that more than half a billion people are infected world wide [1]. *E. histolytica* is an ancestral protozoan organism that evolved shortly after the branching of pro- and eu-karyotes [2,3]. Therefore it possesses some ancient metabolic pathways that differ substantially from those of higher eukaryotes. Although the same intermediates are found, several steps in *E. histolytica* glycolysis are catalysed by enzymes that use unusual cofactors. These enzymes include a pyrophosphate-dependent phosphofructokinase and a GDP-dependent phosphoglycerate kinase. Another peculiarity of the *E. histolytica* glycolytic pathway is the absence of a pyruvate kinase. It is replaced by a complex system consisting of pyruvate orthophosphate dikinase, phosphoenolpyruvate carboxytransphosphorylase, malate dehydrogenase and malate dehydrogenase (decarboxylating). These enzymes accomplish the conversion of phosphoenolpyruvate into pyruvate, which is subsequently oxidatively decarboxylated to acetyl-CoA. As the terminal cytochrome oxidase system is absent from *E. histolytica*, other pathways are necessary to generate oxidized nicotinamide nucleotides. Under anaerobic conditions, reducing equivalents [NAD(P)$^+$] are generated by sequential reduction of acetyl-CoA to acetaldehyde and ethanol [4–6]. Acetyl-CoA is first converted into an enzyme-bound thiohemiacetal by an acetaldehyde dehydrogenase (ACDH; EC 1.2.1.10). The enzyme-bound thiohemiacetal is subsequently reduced by an NAD$^+$-dependent alcohol dehydrogenase (NAD$^+$-ADH; EC 1.1.1.1). Previous studies suggested that both activities reside on a single protein [7], but the protein has not been purified and characterized in detail.

The putative bifunctional activity of the amoebic ACDH/ADH implies structural divergence from human ADH. This opens up opportunities for the development of specific inhibitors, which might be useful for antiparasitic chemotherapy.

Here we report the purification, general properties and primary structure of the NAD$^+$-dependent ACDH/ADH of *E. histolytica*.

MATERIALS AND METHODS

Enzyme assays

An Uvicon spectrophotometer was used for all enzyme assays, which were carried out in a final volume of 1 ml. The standard assay for NAD$^+$-dependent ADH was performed in the presence of 50 mM glycine/NaOH, pH 9.5, 0.2 mM NAD$^+$ and 0.1 M ethanol. Alternatively ADH activity was determined using 50 mM potassium phosphate buffer, pH 6.5, containing 0.2 mM NADH and 0.5 mM acetaldehyde. ACDH activity was determined in 0.1 M Mops/KOH buffer, pH 7.5, containing 0.4 mM NADH and 0.2 mM acetyl-CoA. The rate of change in absorbance was determined at 340 nm ($\epsilon = 6.22 \times 10^3$ M$^{-1}\cdot$cm^{-1}). One unit of enzyme activity was defined as that which consumes 1 μmol of NADH or NAD$^+$/min. Values are expressed as means of at least two independent experiments. For determination of the kinetic parameters, 5 μg of the purified enzyme was used in each assay. The substrate concentrations for NAD$^+$ and NADH ranged from 0.05 to 1 mM, for acetaldehyde from 0.1 to 20 mM, for ethanol from 0.5 to 250 mM and for acetyl-CoA from 0.1 to 2 mM. K_m values were determined using the Lineweaver–Burk plot.

Protein purification

All purification procedures were performed on ice at 4 °C. ADH and ACDH activities were assayed immediately after each purification step, and active material was stored at −20 °C. Samples of active fractions were analysed by SDS/PAGE (8% gels) under reducing conditions [8]. Gels were stained with silver

Abbreviations used: ADH, alcohol dehydrogenase; ACDH, acetaldehyde dehydrogenase; ALDH, aldehyde dehydrogenase; PFL, pyruvate formate lyase.

* To whom correspondence should be addressed.

The nucleotide sequence reported in this paper has been deposited in the EMBL/GenBank/DDBJ Nucleotide Sequence Databases under the accession number X77132.

nitrate. Protein concentrations were determined as described by Bradford [9] with BSA as standard.

Protein purification was carried out from trophozoite lysates of the *E. histolytica* isolate HM:1-IMSS cultured axenically in TYI-S-33 medium [10]. About 3×10^8 cells at late-exponential growth phase were harvested by chilling on ice for 10 min and centrifuged at 430 *g* at 4 °C for 5 min. The resulting pellet was washed twice in PBS, freeze–thawed five times in solid CO_2/ethanol, and sedimented by centrifugation at 150000 *g* at 4 °C for 40 min. The 150000 *g* supernatant was passed in two batches of 8 ml, containing 256 mg of protein each, over a HiLoad 26/60 Superdex 200 f.p.l.c. column (Pharmacia, Uppsala, Sweden) using 20 mM Tris/HCl buffer, pH 7.5. Fractions containing the majority of NAD^+-dependent ADH activity were pooled and applied in a single batch of 36 ml containing 72 mg of protein to a Mono Q anion-exchange column (Pharmacia). The column was equilibrated with 20 mM Tris/HCl buffer, pH 7.5. Adsorbed proteins were eluted by washing with the same buffer (40 ml) and subsequently with an NaCl gradient from 0 to 200 mM (160 ml) and finally by washing with 500 mM NaCl (40 ml). A Blue Sepharose CL-6B affinity column (5 ml bed volume; Sigma, Deisenhofen, Germany) equilibrated with 20 mM Tris/HCl, pH 7.5, was used for the last purification step. The pooled active fractions of the Mono Q anion-exchange column were diluted 1:5 with 20 mM Tris/HCl, pH 7.5, and applied to the column, which was washed with 5 bed vol. of the Tris/HCl buffer. Elution was accomplished by adding the wash buffer containing 10 mM NAD^+ to elute the enzyme at a flow rate of 0.2 ml/min. Fractions containing the majority of ADH activity were pooled.

Amino acid sequencing

The fractions obtained from Mono Q anion-exchange chromatography containing ADH activity were pooled and subjected to reversed-phase h.p.l.c. (Aquapore BU 300 column; Brownlee Laboratories, Santa Clara, CA, U.S.A.) connected with a 130A separation system (Applied Biosystems, Weiterstadt, Germany). Elution was performed with a linear gradient of 0–70 % acetonitrile in water, acidified with 0.1 % trifluoroacetic acid. The flow rate was 0.2 ml/min and 0.2 ml fractions were collected. Fractions were analysed by SDS/PAGE. The fraction containing the protein corresponding to the purified ADH was applied to a gas-phase protein sequencer (model 473A; Applied Biosystems).

Cross-linking

Cross-linking experiments were carried out with the active fractions obtained from the Mono Q anion-exchange chromatography purification step. The bifunctional cross-linker dithiobis(succinimidylpropionate) (Pierce, Rockford, IL, U.S.A.) was added in 20-fold molar excess to the sample and the mixture incubated for 30 min at 4 °C. The protein conjugates were resolved by SDS/PAGE (4 % gels).

Electron microscopy

A Philips CM 10 instrument was used for electron microscopy at an acceleration voltage of 80 kV. Pioloform-coated copper grids (400 mesh) were glow-discharged before samples were adsorbed for 15 s and subsequently negatively stained with 1 % uranyl acetate.

Isolation and sequencing of cDNA and genomic clones

Two oligonucleotide primers ADH-S23 (5′-ATT GCA/T ATT GGA GGA GGA TCA GC) and oligo$(dT)_{18}$ (5′-GAG AGA GAA TTC TTT TTT TTT TTT TTT TTT) were synthesized on an Applied Biosystems DNA synthesizer. The sequence of the ADH-S23 primer was deduced from a region found to be conserved within the amino acid sequences of the AdhE protein from *Escherichia coli* [11], ADH4 from *Saccharomyces cerevisiae* [12] and ADH2 from *Zymomonas mobilis* [13]. The two primers and total DNA obtained from a λZAP cDNA library of the *E. histolytica* isolate HM:IMSS [14] were used for DNA amplification by PCR under standard conditions [15], consisting of 30 cycles each with 1 min of denaturation at 94 °C, 1 min of annealing at 42 °C and 1.5 min of extension at 72 °C.

The amplified DNA was used to screen a cDNA [14] and a genomic library [16] of the *E. histolytica* isolate HM1:IMSS, both constructed in the λZAP phage vector. Hybridizing phages were isolated, and the plasmids were released according to the manufacturer's recommendations (Strategene, Heidelberg, Germany). Selected inserts were sequenced on both strands by the dideoxy-chain termination method [17].

Northern- and Southern-blot analysis

Total *E. histolytica* RNA and DNA were isolated from trophozoites of the isolate HM:1-MSS as previously described [18]. Southern- and Northern-blot analyses were performed according to published procedures [19], using 10 μg of DNA and RNA respectively. Blots were hybridized with the radiolabelled probe using the Prime-a-Gene Labelling System (Promega, Madison, WI, U.S.A.).

RESULTS

Purification of *E. histolytica* ACDH/ADH

NAD^+-dependent ACDH/ADH of *E. histolytica* (EhADH2) was purified by three successive chromatography steps (gel filtration through Superdex 200, anion exchange on Mono Q and a Blue Sepharose affinity column) resulting in a final recovery of 2.8 % of NAD^+-dependent ADH activity and a 71-fold purification (Table 1). SDS/PAGE analysis of the active fractions after Mono Q and Blue Sepharose chromatography revealed a highly enriched protein with a molecular mass of 95 kDa (Figure 1). From previous studies it was suggested that the amoebic NAD^+-dependent ADH is comprised of ADH and ACDH activity. Therefore ACDH activity was monitored in parallel with the ADH activity during purification of the 95 kDa molecule. As summarized in Table 1, the ADH-positive fractions did contain ACDH activity. In addition, the ratio between ADH and ACDH activity was found to be constant after each chromatography step, indicating that the two activities are located on a single molecule.

To determine the N-terminal amino acid sequence of EhADH2, the 95 kDa molecule within the active Mono-Q fractions was purified by h.p.l.c. and subjected to protein sequencing. Unfortunately, the majority of molecules were revealed to have a blocked N-terminus, therefore only the first four amino acid residues could be determined with certainty resulting in the sequence Asn-Met-Ser-Thr.

Molecular characterization of EhADH2

K_m values

The two enzyme activities of purified EhADH2 were further analysed. ADH activity was measured for the forward and

Table 1 Purification of amoebic ACDH/ADH (ADH2)

Total activity was estimated by measuring NAD^+-dependent ADH and ACDH activity. n.d., Not determined.

Purification step	Total protein (mg)	Total activity (units)		Specific activity (units/mg of protein)		Yield (%)		Purification (fold)		Ratio ADH/ACDH
		ADH	ACDH	ADH	ACDH	ADH	ACDH	ADH	ACDH	
Trophozoite extract	512	2304	973	4.5	1.9	100	100	1	1	2.4
Superdex 200	72	2268	864	31.5	12	98	89	7	6	2.6
Mono Q	6	1400	520	233	87	61	53	52	46	2.7
Blue Sepharose	0.2	64	n.d.	320	n.d.	2.8	n.d.	71	n.d.	n.d.

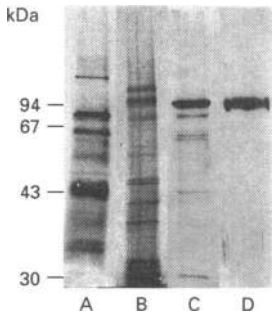

Figure 1 Purification of EhADH2

Protein fractions containing NAD^+-dependent ADH activity at different stages of purification were separated by SDS/PAGE under reducing conditions and visualized by silver staining. Lane A, trophozoite extract (32 μg); lane B, Superdex 200 fraction (2 μg); lane C, Mono Q fraction (0.6 μg); lane D, Blue Sepharose fraction (0.1 μg). Protein standards are indicated on the left.

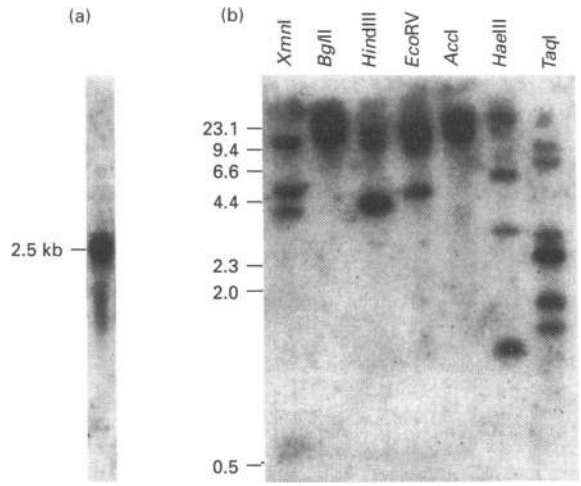

Figure 2 Northern- and Southern-blot analyses

(**a**) Northern blot: 10 μg of *E. histolytica* total RNA was submitted to electrophoresis, blotted and hybridized to a cDNA coding for EhADH2. (**b**) Southern blot: 10 μg of *E. histolytica* genomic DNA was digested to completion with the restriction enzymes as indicated, submitted to electrophoresis, blotted, and hybridized to the cDNA coding for EhADH2. Sizes in kb are indicated on the left.

reverse direction and kinetic studies revealed apparent K_m values for the substrates as follows: acetaldehyde, 0.15 mM; NADH, 0.05 mM; ethanol, 80 mM; NAD^+, 0.15 mM. No reaction was obtained with $NADP^+$ and ethanol as cosubstrates. Furthermore, the purified enzyme exhibited ACDH activity with K_m values of 0.015 mM for acetyl-CoA and 0.18 mM for $NADH^+$.

Primary structure

To determine the primary structure of the EhADH2, corresponding *E. histolytica* cDNA and genomic sequences were analysed. Isolation of these sequences was achieved using an oligonucleotide probe deduced from an amino acid sequence found to be conserved between various NAD^+-dependent ADHs of different prokaryotes and yeast (see the Materials and methods section). The longest cDNA clone was sequenced and revealed an open reading frame of 2616 bp encoding a protein with a calculated molecular mass of 95867 Da. The N-terminal amino acid sequence adjacent to the first encoding methionine was found to be identical with the stretch of sequence obtained by protein sequencing of purified EhADH2.

Northern- and Southern-blot analyses showed a single transcript for EhADH2 of about 2.5 kb encoded by a gene family of multiple copies within the amoebic genome (Figure 2). Analysis of EhADH2 genomic sequences revealed some structural peculiarities common to most *E. histolytica* genes. (i) As far as the cDNA sequence had been obtained it completely matched the genomic sequence implicating a lack of introns for the *E. histolytica adh2* gene. (ii) The sequence motif ATTCA which is known as the transcriptional-start site in various *E. histolytica* genes is located 18 bp upstream of the translation initiation ATG. Furthermore, 28 bp 5′ to the ATTCA element a second consensus motif is found comprising the sequence TATTTAAA. This element is present in nearly all *E. histolytica* genes so far analysed about 30 bp upstream of the start of transcription [20].

The DNA-deduced amino acid sequence of EhADH2 was aligned with ADH and ALDH sequences reported to the EMBL/GenBank/DDBJ Nucleotide Sequence Databases. Over the entire sequence, greatest similarity was found to the trifunctional AdhE protein of *Escherichia coli* (45% amino acid identity; Figure 3), which harbours ADH, ACDH and pyruvate formate lyase (PFL) deactivate activity, and the bifunctional AAD protein of *Clostridium acetobutylicum* (43% amino acid identity), which like the amoebic enzyme possesses ADH and ACDH activity. Significant homology with monofunctional ALDHs was restricted to the N-terminal section and with ADHs to the C-terminal section of EhADH2, suggesting that the two enzymic properties of EhADH2 are located on separate parts of the molecule (Figure 4).

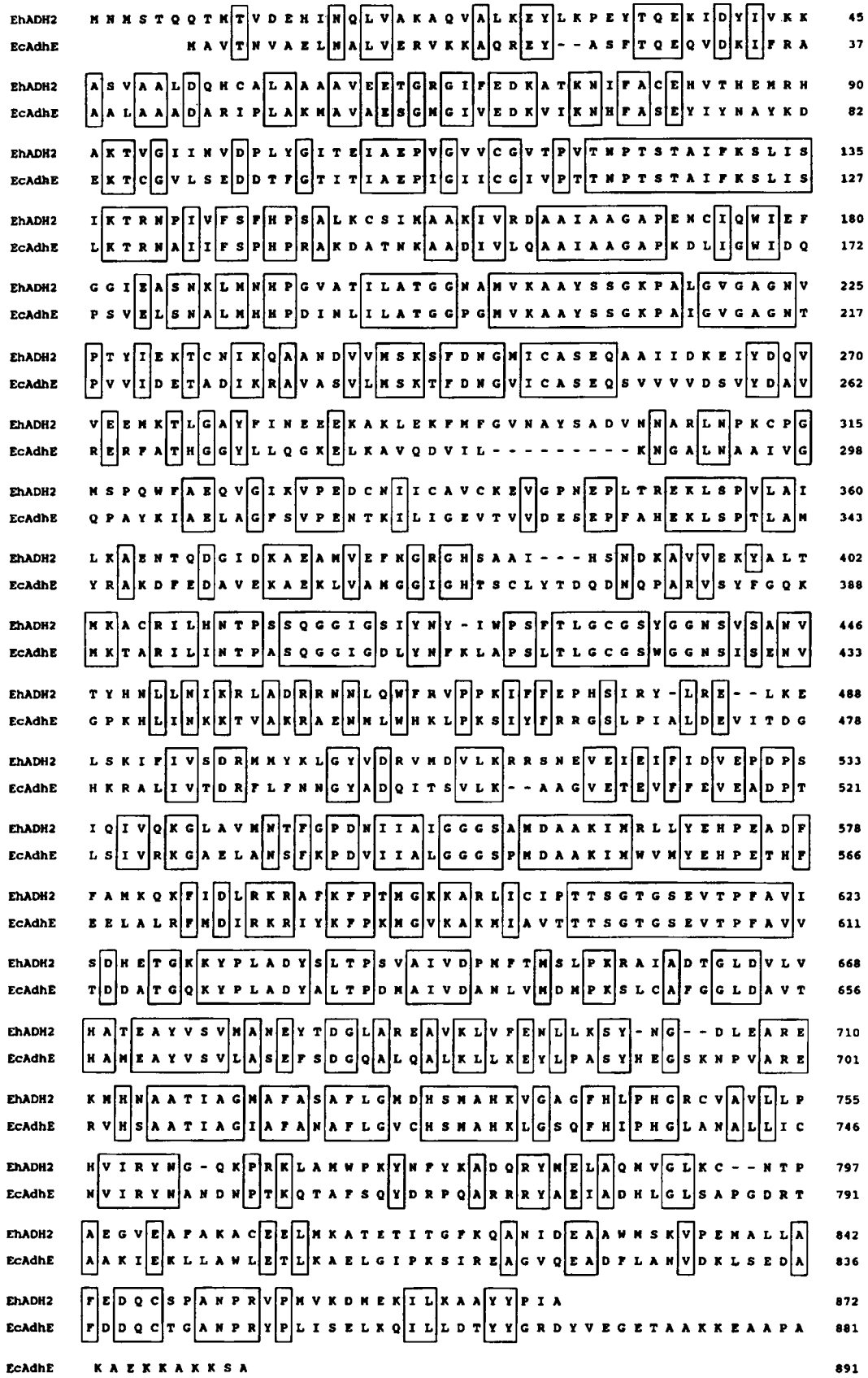

Figure 3 Comparison of the amino acid sequences of EhADH2 from *E. histolytica* and AdhE from *E. coli* [11] (EcAdhE)

Identical residues are boxed. For optimal alignment, gaps were introduced into the sequences.

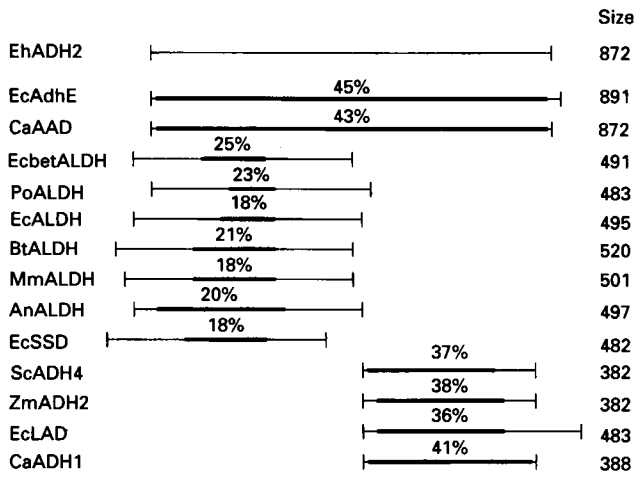

Figure 4 ALDHs and ADHs with similarity to EhADH2

Bars represent ALDHs or ADHs of different species. Areas of substantial homology between these enzymes and EhADH2 are indicated by double lines. Similarities of these areas are expressed as percentage of identical amino acid residues. Abbreviations: EhADH2, *E. histolytica* enzyme (this study); EcAdhE, *E. coli* ADH/ACDH/PFL deactivase [11]; CaAAD, *Cl. acetobutylicum* ALDH/ADH [21]; EcbetALDH, *E. coli* betaine ALDH [22]; PoALDH, *Pseudomonas oleovorans* ALDH [23]; EcALDH, *E. coli* ALDH [24]; BtALDH, *Bos taurus* mitochondrial ALDH [25]; MmALDH, *Mus musculus* cytosolic ALDH [26]; AnALDH, *Aspergillus nidulans* ALDH [27]; EcSSD, *E. coli* succinate semialdehyde dehydrogenase [28]; ScADH4, *Saccharomyces cerevisiae* ADH4 [12]; ZmADH2, *Zymomonas mobilis* ADH2 [13]; EcLAD, *E. coli* lactaldehyde dehydrogenase [29]; CaADH1; *Cl. acetobutylicum* P262 ADH1 [30]. The size of each enzyme expressed as number of comprising amino acid residues is shown on the right.

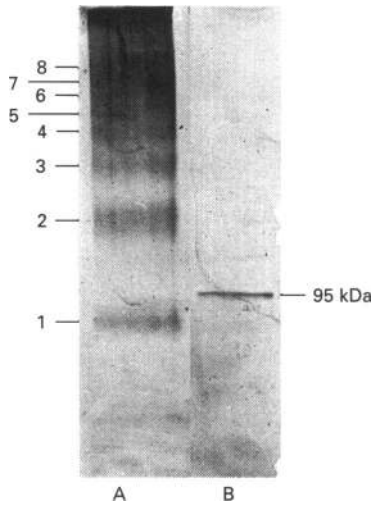

Figure 5 Oligomeric organization of EhADH2 detected by chemical cross-linking

Purified EhADH2 was incubated with a 20-fold molar excess of dithiobis (succinimidylpropionate) for 30 min at 4 °C. The protein conjugates were resolved by SDS/PAGE (4% gels) under non-reducing (lane A) or reducing (lane B) conditions and visualized by silver staining. Numbers denote the numbers of cross-linked protomers of 95 kDa.

Molecular organization

EhADH2 migrates as a single 95 kDa protein band on SDS/PAGE. On the other hand, gel filtration on an f.p.l.c. Superdex 200 column revealed a molecular mass for the native enzyme greater than 200 kDa. Cross-linking experiments with dithiobis (succinimidylpropionate) resulted in the formation of a ladder of homopolymeric peptides (Figure 5). This is in agreement with the rod-forming association of more than 20 protomers in the native EhADH2 protein directly visualized by negative-staining electron microscopy. Rod lengths of 50–120 nm overall were found most, consisting of clearly discernible protomers about 7 nm in length (Figure 6).

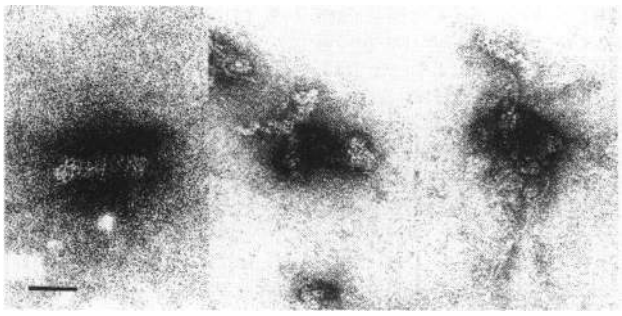

Figure 6 Electron micrograph of negatively stained EhADH2

Purified native EhADH2 was adsorbed to copper grids, negatively stained with uranyl acetate and subjected to electron microscopy. The depicted specimens are representative of most of the molecules observed (size distribution from 50 to 120 nm in length). The bar indicates 50 nm.

DISCUSSION

Two different ADHs have previously been identified in the protozoan parasite *E. histolytica*, the $NADP^+$-dependent EhADH1 and the NAD^+-dependent EhADH2 [7,31]. Although both enzymes might catalyse the final reaction in amoebic glycolysis, the role of EhADH1 is somewhat uncertain. It has a much higher affinity for secondary than primary alcohols [31], suggesting that, under physiological conditions, it is of minor importance in amoebic glycolysis [32]. On the other hand, EhADH2 prefers primary alcohols and in addition harbours ACDH activity [7]. Therefore it would appear to be one of the key enzymes of amoebic glycolysis, as it should catalyse the conversion of acetyl-CoA into enzyme-bound thiohemiacetal and subsequently ethanol.

In an attempt to analyse this enzyme in more detail, we purified and characterized EhADH2. Our results confirm the presence of NAD^+-dependent ACDH and ADH activities on a single molecule. Kinetic studies revealed a lower K_m for acetyl-CoA (0.015 mM) than for acetaldehyde (0.15 mM) and a relatively high K_m of 80 mM for ethanol, which strongly suggests that EhADH2 indeed functions in the direction of ethanol formation.

So far, only two polypeptides of prokaryotic origin have been identified that possess ACDH and ADH activity, the *Cl. acetobutylicum* AAD [23] and the *E. coli* AdhE [11]. Both were found to share striking sequence similarity to EhADH2. Like the amoebic enzyme, AAD consists of 872 amino acid residues whereas AdhE has an additional 19 residues. Besides ACDH and ADH activity the *E. coli* polypeptide also contains PFL deactivase activity. This enzyme catalyses the cleavage of pyruvate to acetyl-CoA and formate [33]. In *E. histolytica*, there is no evidence for the presence of PFL deactivase activity, as pyruvate is only reduced to ethanol and acetate [5].

The N-terminal part of EhADH2 showed weak homology with various ALDHs of different species. Striking similarity was

restricted to a stretch of about 170 amino acid residues with amino acid identities of about 20%. Other regions of high similarity between various ALDHs did not correspond to any sequences of EhADH2, AAD or AdhE.

In contrast with the weak homology of the N-terminal section of EhADH2 to ALDHs, the C-terminal portion of the molecule was found to be highly conserved among various ADHs. Within this portion, a sequence motif is located containing three consecutive glycine residues (position 555). This motif is highly conserved among all NAD^+-dependent ADHs and is also present within other NAD^+-dependent enzymes [34–36], suggesting that it might be involved in NAD^+ binding.

The comparison of primary sequences does not give sufficient information as to whether ACDH and ADH activity are located on separate non-overlapping domains of EhADH2 or whether they are composed of higher structures of the molecule. However, the high similarity of EhADH2 to *E. coli* AdhE strongly suggests a similar functional organization of the *E. histolytica* enzyme. This is underlined by our cross-linking and ultrastructural analyses of EhADH2. A comparison of these results with those reported for AdhE [33] provided evidence that both enzymes are homopolymeric peptides composed of more than 20 protomers associated in a helical rod-like structure. Chymotryptic digestion of AdhE revealed that ADH activity is located within a continuous stretch of sequence, whereas ACDH activity is not [33]. On the basis of homology with this stretch of sequence, we assume that EhADH2 harbours ADH activity between amino acid residues 420 and 770.

The presence of an NAD^+-dependent ACDH/ADH in *E. histolytica*, which until now has only been found in prokaryotic organisms, supports the assumption that this organism belongs to a very early branch of eukaryotic evolution before symbiosis with protomitochondria occurred [3]. This is in line with the occurrence of PP_i-dependent glycolysis [6], and the primary structure of other *E. histolytica* proteins, such as elongation factor 1α [3], iron-containing superoxide dismutase [14] and pyruvate phosphate dikinase [37].

Metronidazole is the most widely used drug for treatment of anaerobic protozoan infections. Considering the reports on resistance to metronidazole in *Entamoeba*, *Giardia* and *Trichomonas*, alternative drugs need to be found [38–41]. Unique enzymes such as EhADH2 are rational targets for chemotherapy, as they are essential for the parasite and specifically tailored inhibitors against them should be non-toxic to the host. Our characterization of EhADH2 might provide the basis for the development of such inhibitors.

Note added in proof (received 22 August 1994)

Some of the biochemical properties and the primary structure of ELADH2 have been reported by Yang et al. [42].

We thank K. Lingelbach for critical reading of the manuscript, M. Denart for skilful technical assistance and C. Schmetz for electron-microscopic analysis. This work was supported by the Bundesministerium für Forschung und Technologie.

Received 15 March 1994/13 May 1994; accepted 26 May 1994

REFERENCES

1 Walsh, J. A. (1986) Res. Infect. Dis. **8**, 228–238
2 Sogin, M. L., Hinkle, G. and Leipe, D. D. (1993) Nature (London) **362**, 795
3 Hasegawa, M., Hashimito, T., Adachi, J., Iwabe, N. and Miyate, T. (1993) J. Mol. Evol. **36**, 380–388
4 Reeves, R. R. (1984) Adv. Parasitol. **23**, 105–142
5 Müller, M. (1988) Annu. Rev. Microbiol. **42**, 465–488
6 Mertens, E. (1993) Parasitol. Today **9**, 122–127
7 Lo, H.-S. and Reeves, R. R. (1978) Biochem. J. **171**, 225–230
8 Laemmli, U. K. (1970) Nature (London) **227**, 680–685
9 Bradford, M. M. (1976) Anal. Biochem. **166**, 368–379
10 Diamond, L. S., Harlow, D. R. and Cunnick, C. C. (1978) Trans. R. Soc. Trop. Med. Hyg. **72**, 431–432
11 Goodlove, P. E., Cunningham, P. R., Parker, J. and Clark, D. P. (1989) Gene **85**, 209–214
12 Williamson, V. M. and Paquin, C. E. (1987) Mol. Gen. Genet. **209**, 374–381
13 Conway, T., Sewell, G. W., Osman, Y. A. and Ingram, L. O. (1987) J. Bacteriol. **169**, 2591–2597
14 Tannich, E., Bruchhaus, I., Walter, R. D. and Horstmann, R. D. (1991) Mol. Biochem. Parasitol. **49**, 61–72
15 Saiki, R. K., Gelfand, D. H., Stoffel, S., Scharf, S. J., Higuchi, R., Horn, G. T., Mullis, K. B. and Erlich, H. A. (1988) Science **230**, 487–491
16 Tannich, E., Nickel, R., Buss, H. and Horstmann, R. D. (1992) Mol. Biochem. Parasitol. **54**, 109–112
17 Sanger, F., Nicklen, S. and Coulson, A. R. (1977) Proc. Natl. Acad. Sci. U.S.A. **74**, 5463–5467
18 Tannich, E., Horstmann, R. D., Knobloch, J. and Arnold, H. H. (1989) Proc. Natl. Acad. Sci. U.S.A. **86**, 5118–5122
19 Sambrook, J., Fritsch, E. F. and Maniatis, T. (1989) Molecular Cloning: A Laboratory Manual, 2nd edn., Cold Spring Harbor Laboratory Press, Cold Spring Harbor, NY
20 Bruchhaus, I., Leippe, M., Lioutas, C. and Tannich, E. (1993) DNA Cell Biol. **12**, 925–933
21 Nair, R. V., Bennett, G. N. and Papoutsakis, E. T. (1994) J. Bacteriol. **176**, 871–885
22 Boyd, L. A., Adam, L., Pelcher, L. E., McHughen, A., Hirji, R. and Selvaraj, G. (1991) Gene **103**, 45–52
23 Kok, M., Oldenhuis, R., van der Linden, M. P. G., Meulenberg, C. H. C., Kingma, J. and Witholt, B. (1989) J. Biol. Chem. **264**, 5442–5451
24 Heim, R. and Strehler, E. E. (1991) Gene **99**, 15–23
25 Guan, K. and Weiner, H. (1990) Arch. Biochem. Biophys. **277**, 351–360
26 Rongnoparut, P. and Weaver, S. (1991) Gene **101**, 261–265
27 Pickett, M., Gwynne, D. I., Buxton, F. P., Elliott, R., Davies, R. W., Lockington, R. A., Scazzocchio, C. and Sealy-Lewis, H. M. (1987) Gene **51**, 217–226
28 Niegeman, E., Schulz, A. and Bartsch, K. (1992) SwissProt accession no. P25526
29 Hidalgo, E., Chen, Y.-M., Lin, E. C. C. and Aguilar, J. (1991) J. Bacteriol. **173**, 6118–6123
30 Youngleson, J. S., Jones, W. A., Jones, D. T. and Woods, D. R. (1989) Gene **78**, 355–364
31 Lo, H.-S. and Chang, C.-J. (1982) J. Parasitol. **68**, 372–377
32 Fairlamb, A. H. (1989) Parasitology **11**, S93–S112
33 Kessler, D., Herth, W. and Knappe, J. (1992) J. Biol. Chem. **267**, 18073–18079
34 Tartaglia, L. A., Storz, G., Brodsky, M. H. Lai, A. and Ames, B. N. (1990) J. Biol. Chem. **265**, 10535–10540
35 Mathieu, I., Meyer, J. and Moulis, J.-M. (1992) Biochem. J. **285**, 255–262
36 Niimuru, Y., Ohnishi, K., Yarita, Y., Hidaka, M., Masaki, H., Ushimura, T., Suzuki, H., Kozaki, M. and Uozumi, T. (1993) J. Bacteriol. **175**, 7945–7950
37 Bruchhaus, I. and Tannich, E. (1993) Mol. Biochem. Parsitol. **62**, 153–156
38 Müller, M. (1986) Biochem. Pharmacol. **35**, 37–41
39 Townson, S. M., Laqua, H., Upcroft, P., Boreham, P. F. L. and Upcroft, J. A. (1992) Trans. R. Soc. Trop. Med. Hyg. **86**, 521–522
40 Ellis, J. E. W., Wingfield, J. M., Cole, D., Boreman, P. F. L. and Lloyd, D. (1993) Int. J. Parasitol. **23**, 35–39
41 Kulda, J., Tachezy, J. and Cerkasovova, A. (1993) J. Euk. Microbiol. **40**, 262–269
42 Yang, W., Li, E., Tian, K. and Stanley, S. L., Jr. (1994) Mol. Biochem. Parasitol. **64**, 253–260